

# Hubble parameter data constraints on dark energy

Yun Chen\*

*Department of Astronomy, Beijing Normal University, Beijing 100875, China and  
Department of Physics, Kansas State University, 116 Cardwell Hall, Manhattan, KS 66506, USA*

Bharat Ratra†

*Department of Physics, Kansas State University, 116 Cardwell Hall, Manhattan, KS 66506, USA  
(Dated: February 24, 2024)*

We use Hubble parameter versus redshift data from Stern et al. [1] and Gaztañaga et al. [2] to place constraints on model parameters of constant and time-evolving dark energy cosmological models. These constraints are consistent with (through not as restrictive as) those derived from supernova Type Ia magnitude-redshift data. However, they are more restrictive than those derived from galaxy cluster angular diameter distance, and comparable with those from gamma-ray burst and lookback time data. A joint analysis of the Hubble parameter data with more restrictive baryon acoustic oscillation peak length scale and supernova Type Ia apparent magnitude data favors a spatially-flat cosmological model currently dominated by a time-independent cosmological constant but does not exclude time-varying dark energy.

PACS numbers: 95.36.+x, 98.80.-k

## I. INTRODUCTION

It is well-established that the Universe is currently undergoing accelerated cosmological expansion. Observational evidence for the accelerated expansion comes from supernova Type Ia (SNIa) apparent magnitude measurements as a function of redshift [3, 4], cosmic microwave background (CMB) anisotropy data [5] combined with low estimates of the cosmological mass density [6], and baryon acoustic oscillation (BAO) peak length scale estimates [2, 7, 8].

The underlying mechanism responsible for this accelerated expansion is not yet well characterized. The “standard” general relativistic model of cosmology has an energy budget that is currently dominated by far by dark energy, a negative-pressure substance that powers the accelerated expansion. (Another possibility is that the above observations are a manifestation of the breakdown of general relativity on large cosmological length scales. In this paper we assume that general relativity provides an adequate description of gravitation on cosmological length scales.) Dark energy can vary weakly in space and evolve slowly in time, though current data are consistent with it being a cosmological constant. For recent reviews see [9].

There are many dark energy models under discussion (for recent discussions see [10], and references therein). The current “standard” model is the  $\Lambda$ CDM model [11] where the accelerated cosmological expansion is powered by Einstein’s cosmological constant,  $\Lambda$ , a spatially homogeneous fluid with equation of state parameter  $\omega_\Lambda = p_\Lambda/\rho_\Lambda = -1$  (where  $p_\Lambda$  and  $\rho_\Lambda$  are the fluid pressure and energy density). In this model the cosmological energy budget is dominated by far by  $\rho_\Lambda$ , with cold dark matter (CDM) being the second largest contributor. The  $\Lambda$ CDM model provides a reasonable fit to most observational constraints, although the “standard” CDM structure formation model might be in some observational trouble (see, e.g., [12]). In addition, the  $\Lambda$ CDM model raises some puzzling conceptual questions.

If the dark energy density slowly decreased in time (rather than remaining constant like  $\rho_\Lambda$ ), the energy densities of dark energy and nonrelativistic matter (CDM and baryons) would remain comparable for a longer period of time, and so alleviate what has become known as the  $\Lambda$ CDM coincidence puzzle. In addition, a slowly decreasing effective dark energy density, based on a more fundamental physics model that is applicable at an energy density scale much larger than an meV, could result in the current observed dark energy density scale of order an meV through gradual decrease over the long lifetime of the Universe, another unexplained feature in the context of the  $\Lambda$ CDM model. Thus a slowly decreasing dark energy density could resolve some of the puzzles of the  $\Lambda$ CDM model [13].

The XCDM parametrization is often used to describe a slowly decreasing dark energy density. In this parametrization the dark energy is modeled as a spatially homogeneous ( $X$ ) fluid with an equation of state parameter  $w_X = p_X/\rho_X$ ,

---

\*Electronic address: chenyun@mail.bnu.edu.cn

†Electronic address: ratra@phys.ksu.edu

where  $w_X < -1/3$  is an arbitrary constant and  $p_X$  and  $\rho_X$  are the pressure and energy density of the  $X$ -fluid. When  $w_X = -1$ , the XCDM parametrization reduces to the complete and consistent  $\Lambda$ CDM model. For any other value of  $w_X (< -1/3)$  the XCDM parametrization is incomplete as it cannot describe spatial inhomogeneities (see, e.g., [14]). Here we study the XCDM parametrization only in the spatially-flat cosmological case.

The  $\phi$ CDM model — in which dark energy is modelled as a scalar field  $\phi$  with a gradually decreasing (in  $\phi$ ) potential energy density  $V(\phi)$  — is the simplest complete and consistent model of a slowly decreasing (in time) dark energy density. Here we focus on an inverse power-law potential energy density  $V(\phi) \propto \phi^{-\alpha}$ , where  $\alpha$  is a nonnegative constant [13, 15]. When  $\alpha = 0$  the  $\phi$ CDM model reduces to the corresponding  $\Lambda$ CDM case. Here we only consider the spatially-flat  $\phi$ CDM cosmological model.

It has been known for some time that a spatially-flat  $\Lambda$ CDM model with current energy budget dominated by a constant  $\Lambda$  is largely consistent with most observational constraints (see, e.g., [16, 17]). SNeIa, CMB, and BAO measurements mentioned above indicate that we live in a spatially-flat  $\Lambda$ CDM model with nonrelativistic matter contributing a little less than 30 % of the current cosmological energy budget, with the remaining slightly more than 70 % contributed by a cosmological constant. These three sets of data carry by far the most weight when determining constraints on models and cosmological parameters.

Future data from space missions will significantly tighten the constraints (see, e.g., [18]). However, at present, it is important to determine independent constraints that can be derived from other presently available data sets. While these data are not yet as constraining as the SNeIa, CMB and BAO data, they potentially can reassure us (if they provide constraints consistent with those from the better known data), or if the two sets of constraints are inconsistent this might lead to the discovery of hidden systematic errors or rule out the cosmological model under consideration.

Other data that have been used to constrain cosmological parameters include galaxy cluster gas mass fraction (e.g., [17, 19]), gamma-ray burst luminosity distance (e.g., [20, 21]), large-scale structure (e.g., [22]), strong gravitational lensing (e.g., [23]), and angular size (e.g., [6, 24, 25]) data. While the constraints from these data are less restrictive than those derived from the SNeIa, CMB and BAO data, both types of data result in largely compatible constraints that generally support a currently accelerating cosmological expansion. This gives us confidence that the broad outlines of the “standard” cosmological model are now in place.

Measurements of the Hubble parameter as a function of redshift,  $H(z)$ , have also been used to constrain cosmological parameters (see [26] for a review). A variant of this test uses lookback time data (see, e.g., [27, 28]). Building on the work of [29], Simon et al. [30] used the differential ages of 32 passively evolving galaxies to determine 9  $H(z)$  measurements in the redshift range  $0.09 \leq z \leq 1.75$ . Cosmological constraints derived using these data are described in [31, 32]; more recent references may be traced through [33].

Stern et al. (2010, hereafter S10) [1] extended the Simon et al. [30] sample to 11 measurements of  $H(z)$  in the redshift range  $0.1 \leq z \leq 1.75$ . These data have been used for cosmological tests by Shafieloo & Clarkson [34]. It has become common to augment the S10 data with the Gaztañaga et al. (2009, hereafter G09) [2] estimates of  $H(z)$  determined from line-of-sight BAO peak position observations. These data, listed in Table 1, have also been used to constrain cosmological parameters (see, e.g., [35, 36] and references therein). There are problems with a number of these analyses. Some of them include both the G09 data points at  $z = 0.24$  and  $z = 0.43$  (which we use here), as well as the G09 single summary data point at  $z = 0.34$  that is based on exactly the same data as the two individual points. In addition, a number of these analyses either ignore the G09 systematic errors or incorrectly account for them. We account for the G09 statistical and systematic errors by combining them in quadrature; the G09 data points we list in Table 1 are identical to those used by Ma & Zhang [35] and Zhang et al. [26].

In this paper we use the 13 S10 and G09  $H(z)$  measurements listed in Table 1 to constrain the  $\Lambda$ CDM and  $\phi$ CDM models and the XCDM parametrization. The resulting constraints are compatible with those derived using other techniques. We also use these  $H(z)$  data in combination with BAO and SNeIa measurements to jointly constrain cosmological parameters in these models. Adding the  $H(z)$  data tightens the constraints, somewhat significantly in some parts of parameter space for some of the models we study.

Our paper is organized as follows. In Sec. II we present the basic equations of the three dark energy models we study. Constraints from the  $H(z)$  data are derived in Sec. III. In Sec. IV we determine joint constraints on the dark energy parameters from a combination of data sets. We summarize our main conclusions in Sec. V.

## II. BASIC EQUATIONS OF THE DARK ENERGY MODELS

The Friedmann equation of the  $\Lambda$ CDM model with spatial curvature can be written as

$$H^2(z, H_0, \mathbf{p}) = H_0^2 [\Omega_{m0}(1+z)^3 + \Omega_\Lambda + (1 - \Omega_{m0} - \Omega_\Lambda)(1+z)^2], \quad (1)$$

where  $z$  is the redshift,  $H(z, H_0, \mathbf{p})$  is the Hubble parameter,  $H_0$  is the Hubble constant, and the model-parameter set is  $\mathbf{p} = (\Omega_{m0}, \Omega_\Lambda)$  where  $\Omega_{m0}$  is the nonrelativistic (baryonic and cold dark) matter density parameter and  $\Omega_\Lambda$  that

of the cosmological constant. Throughout, the subscript 0 denotes the value of a quantity today. In this paper, the subscripts  $\Lambda$ ,  $X$  and  $\phi$  represent the corresponding quantities of the dark energy component in the  $\Lambda$ CDM, XCDM and  $\phi$ CDM scenarios.

In this work, for computational simplicity, spatial curvature is set to zero in the XCDM and  $\phi$ CDM cases. Then the Friedmann equation for the XCDM parametrization is

$$H^2(z, H_0, \mathbf{p}) = H_0^2 \left[ \Omega_{m0}(1+z)^3 + (1 - \Omega_{m0})(1+z)^{3(1+w_X)} \right], \quad (2)$$

where the model-parameter set is  $\mathbf{p} = (\Omega_{m0}, w_X)$ .

In the  $\phi$ CDM model, the inverse power law potential energy density of the scalar field adopted in this paper is  $V(\phi) = \kappa m_p^2 \phi^{-\alpha}$ , where  $m_p$  is the Planck mass, and  $\alpha$  and  $\kappa$  are non-negative constants [15]. In the spatially-flat case the Friedmann equation of the  $\phi$ CDM model is

$$H^2(z, H_0, \mathbf{p}) = \frac{8\pi}{3m_p^2}(\rho_m + \rho_\phi). \quad (3)$$

Here  $H(z) = \dot{a}/a$  is the Hubble parameter where  $a(t)$  is the cosmological scale factor and an overdot denotes a time derivative. The energy densities of the matter and the scalar field are

$$\rho_m = \frac{m_p^2}{6\pi} a^{-3}, \quad (4)$$

and

$$\rho_\phi = \frac{m_p^2}{32\pi}(\dot{\phi}^2 + \kappa m_p^2 \phi^{-\alpha}), \quad (5)$$

respectively. According to the definition of the dimensionless density parameter, one has

$$\Omega_m(z) = \frac{8\pi\rho_m}{3m_p^2 H^2} = \frac{\rho_m}{\rho_m + \rho_\phi}. \quad (6)$$

The scalar field  $\phi$  obeys the differential equation

$$\ddot{\phi} + 3\frac{\dot{a}}{a}\dot{\phi} - \frac{\kappa\alpha}{2}m_p^2\phi^{-(\alpha+1)} = 0. \quad (7)$$

Using Eqs. (3) and (7), as well as the initial conditions described in [15], one can numerically compute the Hubble parameter  $H(z)$ . In this case the model-parameter set is  $\mathbf{p} = (\Omega_{m0}, \alpha)$ .

### III. CONSTRAINTS FROM THE $H(z)$ DATA

We use the 13  $H(z)$  measurements of S10 and G09 listed in Table 1 to constrain cosmological parameters. We constrain cosmological parameters by minimizing  $\chi_H^2$ ,

$$\chi_H^2(H_0, \mathbf{p}) = \sum_{i=1}^{13} \frac{[H^{\text{th}}(z_i; H_0, \mathbf{p}) - H^{\text{obs}}(z_i)]^2}{\sigma_{H,i}^2}. \quad (8)$$

Here  $z_i$  is the redshift at which  $H(z_i)$  has been measured,  $H^{\text{th}}$  is the predicted value of  $H(z)$  in the cosmological model under consideration and  $H^{\text{obs}}$  is the measured value. From  $\chi_H^2(H_0, \mathbf{p})$  we compute the likelihood function  $L(H_0, \mathbf{p})$ . We then treat  $H_0$  as a nuisance parameter and marginalize over it using a gaussian prior with  $H_0 = 68 \pm 3.5 \text{ km s}^{-1} \text{ Mpc}^{-1}$  [37, 38] to get a likelihood function  $L(\mathbf{p})$  that is a function of only the cosmological parameters of interest. The best-fit parameter values  $p^*$  are those that maximize this likelihood function and the 1, 2 and 3  $\sigma$  constraint contours are the set of cosmological parameters (centered on  $p^*$ ) that enclose 68.27, 95.45 and 99.73 %, respectively, of the probability under the likelihood function.

Figures 1–3 show the constraints from the  $H(z)$  data on the three dark energy models we consider. Not unexpectedly, these show that the  $H(z)$  data fairly tightly restrict one combination of the cosmological parameters while leaving the “orthogonal” combination relatively unconstrained. Comparing these results to those shown in Figs. 1–3 of [32], determined using the 9  $H(z)$  data points of Simon et al. [30], we see that the newer S10 and G09 data result in significantly more restrictive constraints on cosmological parameters. These constraints are comparable with those from gamma-ray burst ([21], Figs. 1–3) and lookback time ([27], Figs. 1–3) data. They are more restrictive than those that follow from galaxy cluster angular diameter distance data ([24], Figs. 1–3).

#### IV. JOINT CONSTRAINTS

Following [24], we derive constraints on cosmological parameters of the three models from a joint analysis of the  $H(z)$  data with the BAO data [7] and Union2 compilation of 557 SNeIa apparent magnitude measurements (covering a redshift range  $0.015 < z < 1.4$ ) from [3].

Figures 4–6 show the constraints on the cosmological parameters for the  $\Lambda$ CDM and  $\phi$ CDM models and the XCDM parametrization from a joint analysis of the BAO and SNeIa data, as well as from a joint analysis of the BAO, SNeIa and  $H(z)$  data. Adding the  $H(z)$  data tightens up the constraints somewhat, most significantly in the  $\Lambda$ CDM case (Fig. 4) and least so for the  $\phi$ CDM model (Fig. 6).

Figures 7–9 display the one-dimensional marginalized distribution probabilities of the cosmological parameters for the three cosmological models considered in this work, derived from a joint analysis of the BAO and SNeIa data, as well as from a joint analysis of the BAO, SNeIa and  $H(z)$  data. The marginalized  $2\sigma$  intervals of the cosmological parameters are presented in Table II.

The combination of BAO and SNeIa data gives tight constraints on the cosmological parameters. Adding the currently-available  $H(z)$  data to the mix does shift the constraint contours, however the effect is significant only in some parts of parameter space for only some of the models we study. While useful, current  $H(z)$  data do not have enough weight to significantly affect the combined BAO and SNeIa results in most parts of model-parameter space. The  $H(z)$  data have a little more weight than currently-available gamma-ray burst luminosity measurements ([21], Figs. 4–6 and 10–12).

In summary, the  $H(z)$  data considered here are very consistent with the predictions of a spatially-flat cosmological model with energy budget dominated by a time-independent cosmological constant. However, the data do not rule out time-evolving dark energy, although they do require that it not vary rapidly.

#### V. CONCLUSION

We have shown that the Hubble parameter versus redshift data from S10 and G09 can give interestingly restrictive constraints on cosmological parameters. The resulting constraints are compatible with those derived from other current data, thus strengthening support for the current “standard” cosmological model. The  $H(z)$  data constraints are approximately as restrictive as those that follow from currently-available gamma-ray burst luminosity data and lookback time observations, and more restrictive than those from currently-available galaxy cluster angular size data. They are, however, much less restrictive than those that follow from a combined analysis of BAO peak length scale and SNeIa apparent magnitude data.

The spatially-flat  $\Lambda$ CDM model, currently dominated by a constant cosmological constant, provides a good fit to the data we have studied here. However, these data do not rule out a time-evolving dark energy.

As discussed in [35], future high- $z$ , high-accuracy  $H(z)$  determinations from BAO observations will likely result in cosmological parameter constraints comparable to those that follow from SNeIa data.

#### Acknowledgments

Yun Chen thanks Data Mania for useful discussions. YC was supported by the China State Scholarship Fund No. 2010604111 and the Ministry of Science and Technology national basic science program (project 973) under grant No. 2007CB815401. BR was supported by DOE grant DEFG03-99EP41093.

- 
- [1] D. Stern, et al. , JCAP 1002 (2010) 008 (S10).
  - [2] E. Gaztañaga, A. Cabré, L. Hui, MNRAS 399 (2009) 1663 (G09).
  - [3] R. Amanullah, et al. , Astrophys. J. 716 (2010) 712.
  - [4] A. Shafieloo, V. Sahni, A. A. Starobinsky, Phys. Rev. D 80 (2009) 101301;  
T. Holsclaw, et al. , Phys. Rev. Lett. 105 (2010) 241302;  
J. Guy, et al. , arXiv:1010.4743.
  - [5] B. Ratra, et al. , Astrophys. J. 517 (1999) 549;  
S. Podariu, et al. . Astrophys. J. 559 (2001) 9;  
E. Komatsu, et al. , Astrophys. J. Suppl. 180 (2009) 330;  
E. Komatsu, et al. , Astrophys. J. Suppl. 192 (2011) 18.
  - [6] G. Chen, B. Ratra, PASP 115 (2003) 1143.

- [7] W. J. Percival, et al. , MNRAS 401 (2010) 2148;
- [8] L. Samushia, B. Ratra, Astrophys. J. 701 (2009) 1373;  
Y. Wang, Mod. Phys. Lett. A 25 (2009) 3093.
- [9] B. Ratra, M. S. Vogeley, PASP 120 (2008) 235;  
M. Bartelmann, Rev. Mod. Phys. 82 (2010) 331;  
Y.-F. Cai, et al. , Phys. Rept. 493 (2010) 1;  
S. Capozziello, M. De Laurentis, V. Faraoni, arXiv:0904.4672;  
P. Brax, arXiv:0912.3610;  
J.-P. Uzan, arXiv:0912.5452;  
A. De Felice, S. Tsujikawa, Living Rev. Rel. 13 (2010) 3;  
M. Li, et al. , arXiv:1103.5870.
- [10] K. Hirano, Z. Komiya, Int. J. Mod. Phys. D 20 (2011) 1;  
S.-H. Chen, et al. , Phys. Rev. D 83 (2011) 023508;  
X. Chen, et al. , Phys. Lett. B 695 (2011) 30;  
A. Ali, R. Gannouji, M. Sami, Phys. Rev. D 82 (2010) 103012;  
B. Novosyadlyj, et al. , Phys. Rev. D 82 (2010) 103008;  
T. Harko, F. S. N. Lobo, Eur. Phys. J. C 70 (2010) 373.
- [11] P. J. E. Peebles, ApJ 284 (1984) 439.
- [12] P. J. E. Peebles, B. Ratra, Rev. Mod. Phys. 75 (2003) 559;  
L. Perivolaropoulos, J. Phys. Conf. Ser. 222 (2010) 012024.
- [13] B. Ratra, P. J. E. Peebles, Phys. Rev. D 37 (1988) 3406.
- [14] B. Ratra, Phys. Rev. D 43 (1991) 3802.
- [15] P. J. E. Peebles, B. Ratra, Astrophys. J. 325 (1988) L17.
- [16] H. K. Jassal, J. S. Bagla, T. Padmanabhan, MNRAS 405 (2010) 2639;  
K. M. Wilson, G. Chen, B. Ratra, Mod. Phys. Lett. A 21 (2006) 2197;  
T. M. Davis, et al. , Astrophys. J. 666 (2007) 716.
- [17] S. W. Allen, et al. , MNRAS 383 (2008) 879
- [18] S. Podariu, P. Nugent, B. Ratra, B Astrophys. J. 553 (2001) 39;  
L. Samushia, et al. , MNRAS 410 (2011) 1993;  
Y. Wang, et al. , MNRAS 409 (2010) 737.
- [19] L. Samushia, B. Ratra, Astrophys. J. 680 (2008) L1;  
S. Ettori, et al. , A&A 501 (2009) 61.
- [20] B. E. Schaefer, Astrophys. J. 660 (2010) 16;  
N. Liang, S. N. Zhang, AIP Conf. Proc. 1065 (2008) 367;  
Y. Wang, Phys. Rev. D 78 (2008) 123532.
- [21] L. Samushia, B. Ratra, Astrophys. J. 714 (2010) 1347.
- [22] M. Baldi, arXiv:1005.2188;  
S. Basilakos, M. Plionis, J. Solà, Phys. Rev. D 82 (2010) 083512;  
M. Baldi, V. Pettorino, arXiv:1006.3761;  
C. De Boni, et al. , arXiv:1008.5371.
- [23] K.-H. Chae, et al. , ApJ 607 (2004) L71;  
S. Lee, K.-W. Ng, Phys. Rev. D 76 (2007) 043518;  
M. Yashar, et al. , Phys. Rev. D 79 (2009) 103004;  
M. Biesiada, A. Piórkowska, B. Malec, MNRAS 406 (2010) 1055.
- [24] Y. Chen, B. Ratra, arXiv:1105.5660.
- [25] L. I. Gurvits, K. I. Kellermann, S. Frey, A&A 342 (1999) 378;  
E. J. Guerra, R. A. Daly, L. Wan, Astrophys. J. 544 (2000) 659;  
G. Chen, B. Ratra, ApJ 582 2003 586;  
M. Bonamente, et al. , Astrophys. J. 647 (2006) 25.
- [26] T.-J. Zhang, C. Ma, T. Lan, Adv. Astron. 2010 (2010) 184284.
- [27] L. Samushia, et al. , Phys. Lett. B 693 (2010) 509.
- [28] S. Capozziello, et al. , Phys. Rev. D 70 (2004) 123501;  
N. Pires, Z.-H. Zhu, J. S. Alcaniz, Phys. Rev. D 73 (2006) 123530;  
M. A. Dantas, et al. , Phys. Lett. B 699 (2011) 239.
- [29] R. Jimenez, A. Loeb, Astrophys. J. 573 (2002) 37;  
R. Jimenez, et al. , Astrophys. J. 593 (2003) 622.
- [30] J. Simon, L. Verde, R. Jimenez, Phys. Rev. D 71 (2005) 123001.
- [31] Z.-L. Yi, T.-J. Zhang, Mod. Phys. Lett. A 22 (2007) 41;  
L. Samushia, B. Ratra, Astrophys. J. 650 (2006) L5;  
H. Wei, S.-N. Zhang, Phys. Lett. B 644 (2007) 7;  
P. Wu, H. Yu, Phys. Lett. B 644 (2007) 16;  
A. Kurek, M. Szydlowski, Astrophys. J. 675 (2008) 1;  
H. Zhang, Z.-H. Zhu, JCAP 0803 (2008) 007;  
A. A. Sen, R. J. Scherrer, Phys. Lett. B 659 (2008) 457;

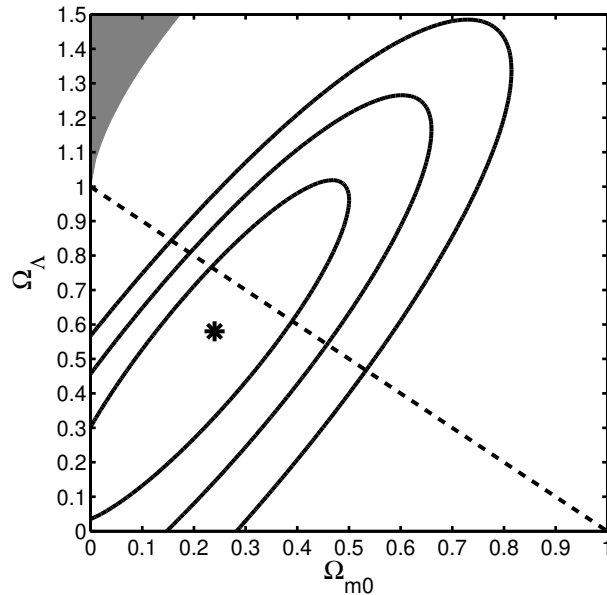


FIG. 1: 1, 2, and 3  $\sigma$  constraint contours for the  $\Lambda$ CDM model from the  $H(z)$  data. The dashed diagonal line corresponds to spatially-flat models and the shaded area in the upper left-hand corner is the region for which there is no big bang. The star marks the best-fit pair  $(\Omega_{m0}, \Omega_{\Lambda}) = (0.24, 0.58)$  with  $\chi^2_{\min} = 10.1$ .

- R. Lazkoz, E. Majerotto, JCAP 0707 (2007) 015.
- [32] L. Samushia, G. Chen, B. Ratra, arXiv:0706.1963.
- [33] Z.-X. Zhai, H.-Y. Wan, T.-J. Zhang, Phys. Lett. B 689 (2010) 8;  
N. Pan, et al. , Class. Quantum Grav. 27 (2010) 155015.
- [34] A. Shafieloo, C. Clarkson, Phys. Rev. D 81 (2010) 083537.
- [35] C. Ma, T.-J. Zhang, Astrophys. J. 730 (2011) 74.
- [36] Y. Wang, L. Xu, Phys. Rev. D 81 (2010) 083523;  
L. Xu, Y. Wang, JCAP 1006 (2010) 002;  
L. Xu, Y. Wang, arXiv:1009.0963;  
L. Xu, J. Lu, JCAP 1003 (2010) 025;  
I. Durán, D. Pavón, W. Zimdahl, JCAP 1007 (2010) 018;  
S. Cao, N. Liang, Z.-H. Zhu, arXiv:1105.6274;  
S. Cao, Z.-H. Zhu, N. Liang, A&A, 529 (2011) A61;  
M. L. Tong, Y. Zhang, Z. W. Fu, Class. Quant. Grav. 28 (2011) 055006;  
D. Adak, A. Bandyopadhyay, D. Majumdar, arXiv:1102.4726.
- [37] G. Chen, J. R. Gott, B. Ratra, PASP 115 (2003) 1269.
- [38] G. Chen, B. Ratra, arXiv:1105.5206.

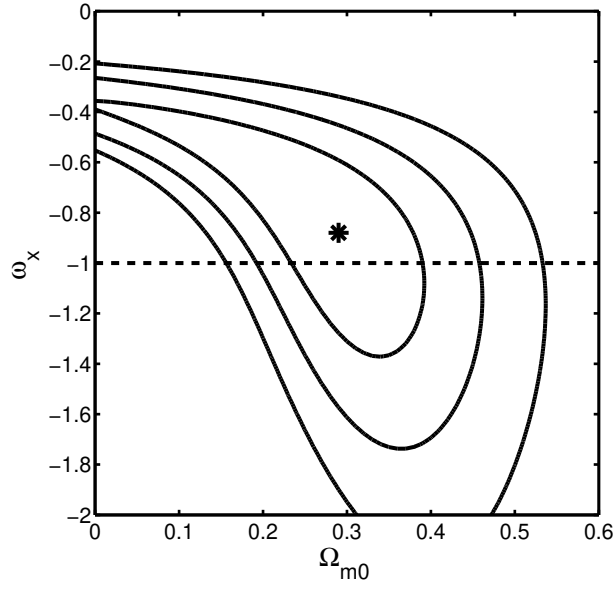


FIG. 2: 1, 2, and 3  $\sigma$  constraint contours for the XCDM parametrization from the  $H(z)$  data. The dashed horizontal line at  $\omega_X = -1$  corresponds to spatially-flat  $\Lambda$ CDM models. The star marks the best-fit pair  $(\Omega_{m0}, \omega_X) = (0.29, -0.88)$  with  $\chi^2_{\min} = 10.1$ .

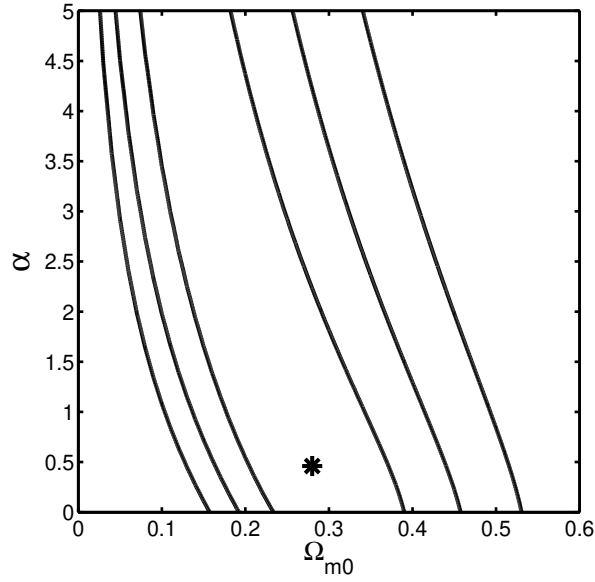


FIG. 3: 1, 2, and 3  $\sigma$  constraint contours for the  $\phi$ CDM model from the  $H(z)$  data. The horizontal axis at  $\alpha = 0$  corresponds to spatially-flat  $\Lambda$ CDM models. The star marks the best-fit pair  $(\Omega_{m0}, \alpha) = (0.28, 0.46)$  with  $\chi^2_{\min} = 10.1$ .

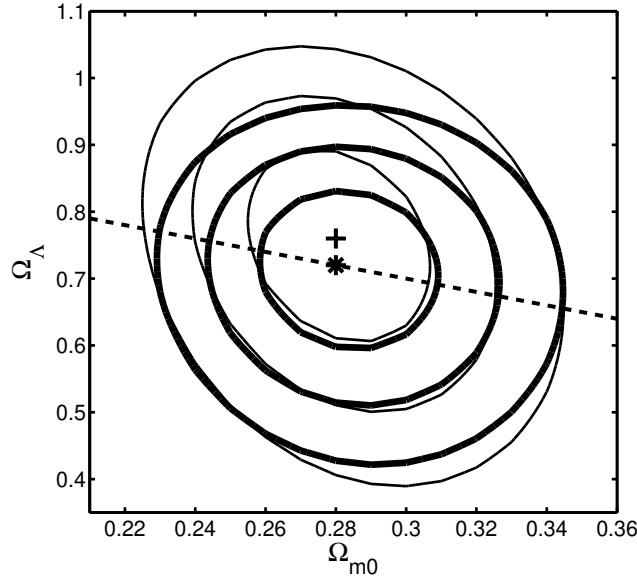


FIG. 4: Thick (thin) solid lines are 1, 2, and 3  $\sigma$  constraint contours for the  $\Lambda$ CDM model from a joint analysis of the BAO and SNeIa (with systematic errors) data, with (and without) the  $H(z)$  data. The cross (“+”) marks the best-fit point determined from the joint sample without the  $H(z)$  data at  $\Omega_{m0} = 0.28$  and  $\Omega_{\Lambda} = 0.76$  with  $\chi^2_{\min} = 531$ . The star (“\*”) marks the best-fit point determined from the joint sample with the  $H(z)$  data at  $\Omega_{m0} = 0.28$  and  $\Omega_{\Lambda} = 0.72$  with  $\chi^2_{\min} = 541$ . The dashed sloping line corresponds to spatially-flat models.

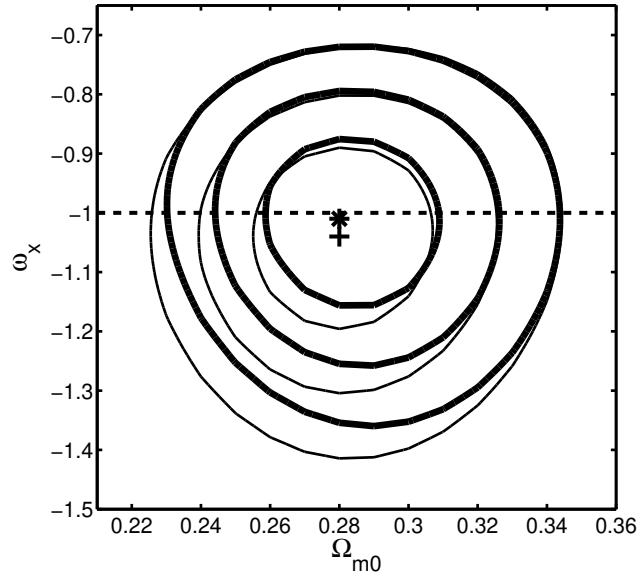


FIG. 5: Thick (thin) solid lines are 1, 2, and 3  $\sigma$  constraint contours for the XCDM parametrization from a joint analysis of the BAO and SNeIa (with systematic errors) data, with (and without) the  $H(z)$  data. The cross (“+”) marks the best-fit point determined from the joint sample without the  $H(z)$  data at  $\Omega_{m0} = 0.28$  and  $\omega_X = -1.04$  with  $\chi^2_{\min} = 531$ . The star (“\*”) marks the best-fit point determined from the joint sample with the  $H(z)$  data at  $\Omega_{m0} = 0.28$  and  $\omega_X = -1.01$  with  $\chi^2_{\min} = 541$ . The dashed horizontal line at  $\omega_X = -1$  corresponds to spatially-flat  $\Lambda$ CDM models.



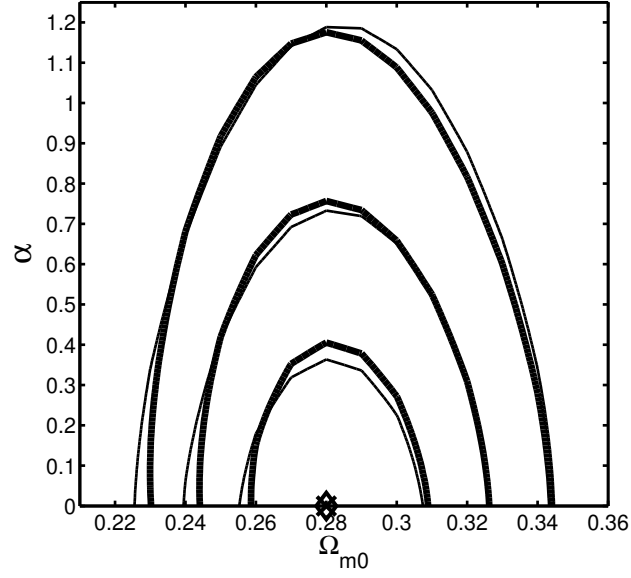


FIG. 6: Thick (thin) solid lines are 1, 2, and 3  $\sigma$  constraint contours for the  $\phi$ CDM model from a joint analysis of the BAO and SNeIa (with systematic errors) data, with (and without) the  $H(z)$  data. The cross (“x”) marks the best-fit point determined from the joint sample without the  $H(z)$  data at  $\Omega_{m0} = 0.28$  and  $\alpha = 0$  with  $\chi^2_{\min} = 531$ . The diamond (“ $\diamond$ ”) marks the best-fit point determined from the joint sample with the  $H(z)$  data at  $\Omega_{m0} = 0.28$  and  $\alpha = 0.0$  with  $\chi^2_{\min} = 541$ . The  $\alpha = 0$  horizontal axis corresponds to spatially-flat  $\Lambda$ CDM models.

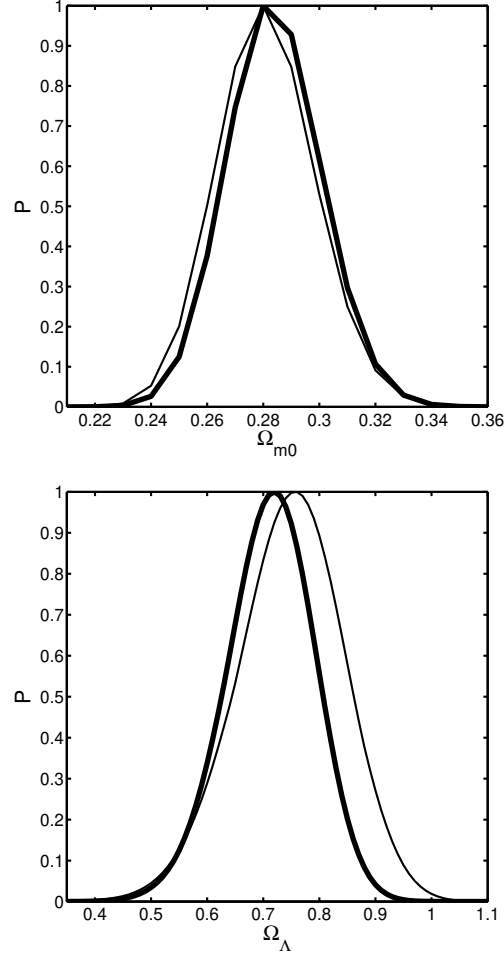


FIG. 7: One-dimensional marginalized distribution probabilities of the cosmological parameters for the LCDM model. Thick (thin) lines are results from a joint analysis of the BAO and SNeIa (with systematic errors) data, with (and without) the  $H(z)$  data.

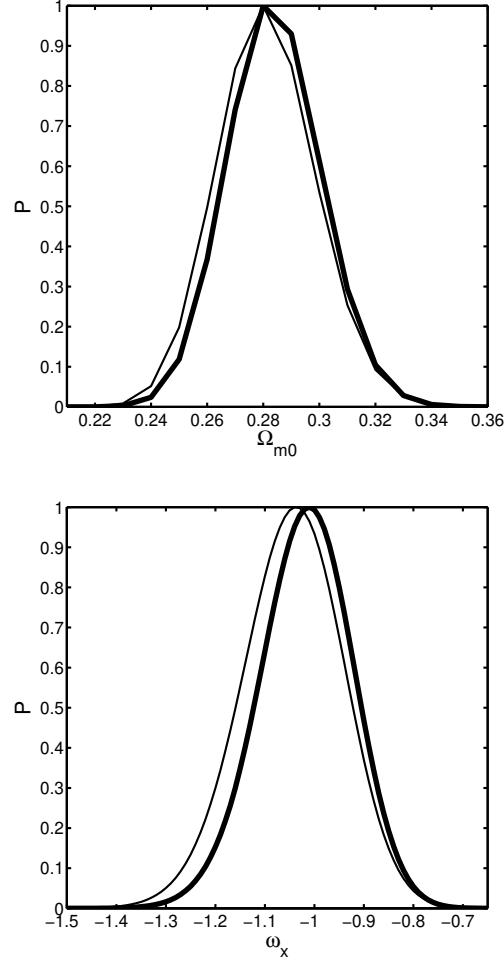


FIG. 8: One-dimensional marginalized distribution probabilities of the cosmological parameters for the XCDM parametrization. Thick (thin) lines are results from a joint analysis of the BAO and SNeIa (with systematic errors) data, with (and without) the  $H(z)$  data.

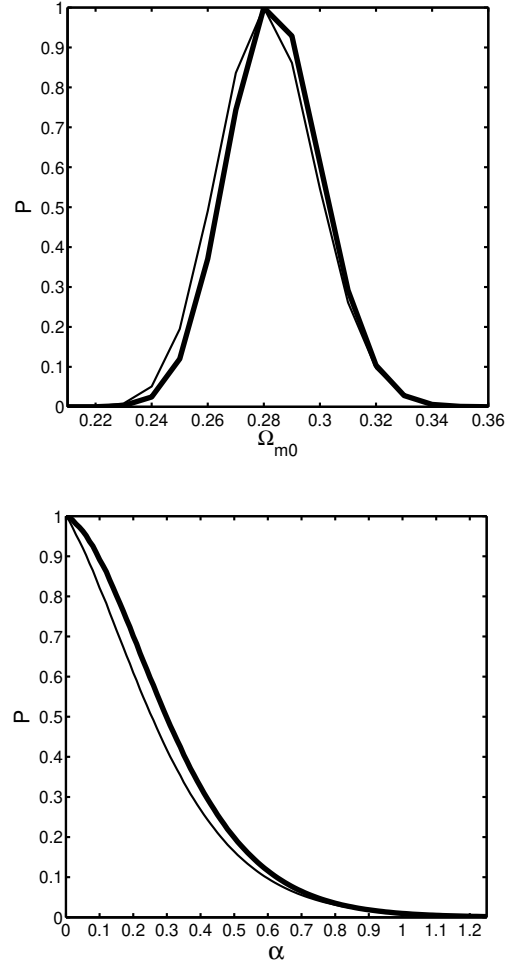


FIG. 9: One-dimensional marginalized distribution probabilities of the cosmological parameters for the  $\phi$ CDM model. Thick (thin) lines are results from a joint analysis of the BAO and SNeIa (with systematic errors) data, with (and without) the  $H(z)$  data.

$z$	$H(z)$	$\sigma_H$
0.1	69	12
0.17	83	8
0.24	79.69	2.65
0.27	77	14
0.4	95	17
0.43	86.45	3.68
0.48	97	60
0.88	90	40
0.9	117	23
1.3	168	17
1.43	177	18
1.53	140	14
1.75	202	40

TABLE I: Hubble parameter versus redshift data from S10 and G09. Where  $H(z)$  and  $\sigma_H$  are in  $\text{km s}^{-1} \text{Mpc}^{-1}$ .

Model	BAO + SNeIa	$H(z)$ + BAO + SNeIa
$\Lambda\text{CDM}$	$0.24 < \Omega_{m0} < 0.33$	$0.24 < \Omega_{m0} < 0.33$
	$0.5 < \Omega_\Lambda < 0.97$	$0.51 < \Omega_\Lambda < 0.9$
$\text{XCDM}$	$0.24 < \Omega_{m0} < 0.33$	$0.24 < \Omega_{m0} < 0.33$
	$-1.30 < \omega_X < -0.80$	$-1.26 < \omega_X < -0.79$
$\phi\text{CDM}$	$0.24 < \Omega_{m0} < 0.33$	$0.24 < \Omega_{m0} < 0.33$
	$0 < \alpha < 0.73$	$0 < \alpha < 0.76$

TABLE II: Two standard deviation bounds on cosmological parameters.